In Situ Electrochemical X-ray Spectromicroscopy Investigation of the Reduction/Reoxidation Dynamics of Ni–Cu Solid Oxide Fuel Cell Anodic Material in Contact with a Cr Interconnect...

ARTICLE *in* THE JOURNAL OF PHYSICAL CHEMISTRY C · MARCH 2012

Impact Factor: 4.77 · DOI: 10.1021/jp208478n

8 AUTHORS, INCLUDING:

Benedetto Bozzini
Università del Salento
259 PUBLICATIONS **2,280** CITATIONS
SEE PROFILE

Mauro Prasciolu
Deutsches Elektronen-Synchrotron
60 PUBLICATIONS **503** CITATIONS
SEE PROFILE

Alexander Trigub
Kurchatov Institute
13 PUBLICATIONS **33** CITATIONS
SEE PROFILE

Maya Kiskinova
Elettra-Sincrotrone Trieste
299 PUBLICATIONS **5,394** CITATIONS
SEE PROFILE

Journal of Power Sources 211 (2012) 71–76

Contents lists available at SciVerse ScienceDirect

Journal of Power Sources

journal homepage: www.elsevier.com/locate/jpowsour

Electrodeposition of manganese oxide from eutectic urea/choline chloride ionic liquid: An in situ study based on soft X-ray spectromicroscopy and visible reflectivity

Benedetto Bozzini [a,*], Alessandra Gianoncelli [b], Burkhard Kaulich [b], Claudio Mele [a], Mauro Prasciolu [c], Maya Kiskinova [b]

[a] Dipartimento di Ingegneria dell'Innovazione, Università del Salento, Via Monteroni, 73100 Lecce, Italy
[b] Elettra – Sincrotrone Trieste S.C.p.A., S.S. 14, km 163.5 in Area Science Park, 34149 Trieste-Basovizza, Italy
[c] CNR-INFM TASC National Laboratory, S.S. 14, km 163.5 in Area Science Park, 34149 Trieste-Basovizza, Italy

ARTICLE INFO

Article history:
Received 17 November 2011
Received in revised form
21 March 2012
Accepted 24 March 2012
Available online 11 April 2012

Keywords:
Manganese oxide
Manganese
Ionic liquid
Electrodeposition
X-ray microspectroscopy
Reflectivity

ABSTRACT

In this work, we describe a novel approach to the fabrication of MnO_2, consisting in Mn electrodeposition from a choline chloride/urea eutectic ionic liquid bath followed by controlled electrochemical oxidation in an aqueous solution. Both electrodeposition and electro-oxidation processes have been studied by electrochemical and in situ spectroelectrochemical approaches. Synchrotron-based soft X-ray scanning microscopy and absorption spectroscopy were used to measure in situ the Mn valence distribution on the electrodes and within the cell. The oxidation process was followed in situ by visible reflectivity measurements: the different stages of the oxidation process could be discriminated dynamically on the basis of relative reflectivity changes. The capacitance of the electrochemically fabricated films has been measured with cyclic voltammetry and electrochemical impedance spectrometry.

1. Introduction

Electrochemical supercapacitors have become a versatile solution to various emerging energy application. They are charge storage devices with greater power density and a longer cycle life than batteries, and a higher energy density compared with conventional capacitors [1]. The most widely used active electrode materials are carbon [2,3], conducting polymers [4,5], noble [6–8] and transition metal-oxides [9–12]. Among these electrode materials, manganese oxide has gained significant interest due to its cheapness, capacitive performance and environmental compatibility [13,14]. Moreover, in the development of energy storage devices, nanostructured electrode materials have attracted great interest, as they show higher capacities and better rates than traditional materials [15,16]. A host of approaches to the fabrication of highly capacitive manganese oxides is documented in the literature, among which fully electrochemical methods are found, based on two alternative routes: anodic oxidation from Mn^{2+} solutions and electrodeposition of Mn followed by controlled oxidation. The quality of the final, oxidised material is strongly dependent on the morphology of the metallic Mn precursor film and it is well known from the literature that Mn electrodeposition from aqueous solutions typically gives rise to incoherent and notably rough films, chiefly owing to the high rate of concurrent hydrogen evolution. For this reason, the use of room temperature ionic liquids (RTIL) as solvents for Mn electrodeposition has been recently proposed, in view of the fabrication of higher-quality material [17–20].

Deep eutectic solvents (DES) represent a class of ionic liquids and refer to the mixture of two solid compounds whose melting temperatures are usually above room temperature but when placed together form a compound that has a melting point lower than room temperature. DES are formed from eutectic mixtures of a quaternary ammonium salt with a hydrogen bond donor species as a carboxylic acid, a glycol or an amine and are known for their ability to dissolve metal salts and oxides as well as organic material such as cellulose. Choline chloride based DES have been successfully assessed for electrodeposition of different metals (Cr, Mn, Cu,

* Corresponding author. Tel.: +39 832 297323; fax: +39 832 297111.
E-mail address: benedetto.bozzini@unisalento.it (B. Bozzini).

0378-7753/$ – see front matter © 2012 Published by Elsevier B.V.
doi:10.1016/j.jpowsour.2012.03.046

Ag, Fe, Zn) [21–24] and alloys (Zn/Cr, Zn/Sn) [25,26] on different substrates.

In the present work we propose the electrochemical fabrication of manganese oxide obtained by oxidation of Mn electrodeposited from a DES based on choline chloride and urea. The electrodeposition process was studied by standard electrochemical methods and by in situ soft X-ray scanning microscopy and absorption spectroscopy. The electrochemical oxidation was monitored by means of in situ VIS reflectivity experiments. The Mn oxide films were characterised in terms of their morphology with scanning electron microscopy and capacitive performance using a combination of electrochemical techniques including cyclic voltammetry and electrochemical impedance spectrometry.

2. Experimental

The ionic liquid formulation was achieved by mixing urea and choline chloride (ChCl) in a 2:1 M ratio and heating to a temperature of 80 °C, with continuous magnetic stirring, until a clear colourless liquid formed. $MnCl_2$ 1 M was then added into the mixture and stirring was continued for 30 min to obtain a homogenous liquid. Electrodeposition was carried out at 25 °C.

Electrochemical measurement (potentiostatic deposition, cyclic voltammetry (CV) and electrochemical impedance spectrometry (EIS)) were carried out with an AMEL 5000 potentiostat/galvanostat connected to a frequency response analyser (Solartron SI 1250). A three-electrode electrochemical cell was employed. The working- (WE) (with an exposed area of 1 cm^2) and counter- (CE 3 cm^2) electrodes were Au wires. An Au wire was also chosen as the quasi-reference electrode (QRE), as customary in the literature [17]. Before each electrochemical measurement or electrodeposition process, the three Au wires were treated as detailed in [27]. CV measurements at 100 mV s^{-1} were performed in order to characterise the pure electrolyte and the Mn bath. Mn thin films were cathodically deposited on Au wire under a nitrogen atmosphere in a glove box, in which the moisture and oxygen contents were maintained below 1 ppm. The deposited films were thoroughly cleaned with acetone and isopropanol, according to [28] and then they were electrochemically oxidised by means of CV in aerated 0.1 M Na_2SO_4 aqueous solution at 25 °C at a scan rate of 25 mV s^{-1}. Growth rates were evaluated gravimetrically with a Sartorius balance having an accuracy of 10^{-5} g. The electrochemical properties of the obtained Mn oxides were investigated in the same solution in two ways: (i) by CV, varying the potential scan rate in the range from 5 to 100 mV s^{-1} and (ii) by means of EIS. In the tests carried out in the aqueous solution the CE was a platinised Ti expanded mesh electrode exhibiting an area of ca. 5 cm^2 and the RE was an AMEL Ag/AgCl (KCl 3 M); potential values are reported vs. Ag/AgCl.

The surface morphology of the samples was examined with a Cambridge Stereoscan scanning electron microscope (SEM).

In situ visible electrochemical reflectance spectroscopy (ERS) measurements were carried out in a cell with a vertical polycrystalline Au disc WE of diameter 5 mm embedded in a Teflon cylindrical holder. The CE and QRE electrodes were Au wires. p-polarised light at an incidence angle of 45° was chosen, in order to emphasise surface information. The spectrometer, optics and control electronics were constructed in our laboratory. Solid state light sources were employed and the wavelength was selected with a grating monochromator, with a spectral resolution of 7 nm and a photodiode detector. In this particular experiment the reflectivity changes as a function of applied potential were directly read from the photodiode preamplifier and could be correlated with the electrochemical conditions, without need of lock-in detection of relative reflectivity variations.

Soft X-ray transmission microscopy (STXM), coupled with micro-spot X-ray absorption spectroscopy (XAS) experiments were performed at the TwinMic beamline of Elettra synchrotron facility (Trieste, Italy) [29,30]. An open electrochemical cell, based on the design proposed and described in detail elsewhere [31,32] was used, but a new geometry was implemented for better control of the current density distribution (Fig. 1). The cell consists of a Si_3N_4 optical window onto which three 40 nm thick Au electrodes – acting as WE, CE and QRE, respectively – were fabricated by Electron Beam Lithography (EBL) direct writing, Au thermal evaporation and standard lift-off. This cell configuration allows to work with an X-ray beam crossing the electrode/electrolyte assembly normally to the optical window: the transmitted X-rays can thus be monitored by the CCD detector placed behind the cell [33,34]. The RTIL was spun on the lithographed electrode assembly, in order to achieve a thickness of 200 nm, optimal for detection of transmitted X-rays and emitted fluorescence signal from the electrodes immersed in the electrolyte. As demonstrated in [31,35–37], using this technique one can obtain simultaneously in situ information on the evolution of the morphology and chemical state of electrodic materials during electrochemical processes.

3. Results and discussion

3.1. Electrodeposition of Mn

The electrodeposition of Mn was studied by standard electrochemical methods (Section 3.1.1), in order to identify the relevant electrochemical process windows as well as the prevailing electrokinetic processes, and by in situ soft X-ray scanning microscopy and absorption spectroscopy (Section 3.1.2), in order to obtain space resolved information in situ regarding the electrode morphology and chemical state of Mn.

3.1.1. Electrochemical measurements

A CV of the Au electrode in 2:1 urea/ChCl is reported in Fig. 2a, showing the extent of the double layer charging region, ranging from ca. 0 V – where the Au oxidation starts - to ca. −1.75 V where the reduction of the IL occurs. The first cathodic-going voltammetric scan in the electrolyte containing $MnCl_2$ 1M is reported in Fig. 2b, showing that Mn reduction takes place at ca. −1.4 V, well within the electrochemical window. Exploratory electrodeposition experiments, followed by controlled oxidation, revealed that the optimal growth condition was at a cathodic potential of −1.7 V for 1 h, yielding a cathodic efficiency of 91 ± 3%. The electrodeposited Mn films were subsequently oxidised electrochemically, as detailed

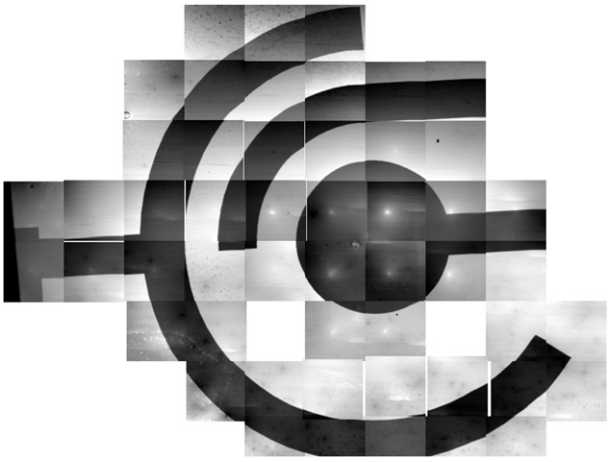

Fig. 1. STXM images of the cell with Au anode and cathode in pristine conditions.

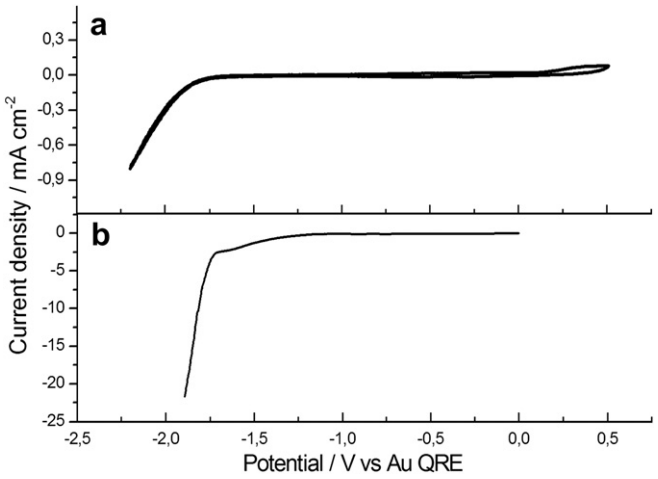

Fig. 2. (a) Cyclic voltammogram of an Au electrode in 2:1 urea/ChCl. (b) Cathodic linear sweep voltammetry measured with the same electrode in the same electrolyte with the addition of $MnCl_2$ 1 M. Potential scan rate of 100 mV s^{-1}.

in Section 3.2, causing a weight gain of 145 ± 5%, corresponding to a mass for unit area of 110 ± 7 μg cm^{-2}. For material characterisation, electrodeposited samples were produced in triplicate.

3.1.2. STXM imaging and XAS spectromicroscopy

In order to achieve a more insightful understanding of the electrodeposition process, the anode, cathode and electrolyte regions of the thin-layer electrochemical cell, described in Section 2, were characterised by means of STXM and XAS spectromicroscopy.

The electrochemically active areas of cathode and anode were imaged by STXM under the following conditions: (i) at OCP before application of potential (i.e. pristine Au electrode conditions) (Fig. 1) and (ii) after the application of a cathodic potential of −1.7 V for 2 min (Fig. 3a). Comparing the images reported in Figs. 1 and 3a the formation of anodic and cathodic electrodeposits can be noticed, both on the electrodes and projecting into the electrolyte in the vicinity of the electrodes. Fig. 3b shows a representative set of Mn L-edge XAS spectra, measured in the selected points of the cathode, anode and electrolyte, indicated in Fig. 3a. The peak positions, lineshapes and L_3/L_2 intensity ratios of the Mn $L_{2,3}$ spectra are the fingerprints of the Mn oxidation state in the analysed locations. By increasing the valency the spectra shift to higher energy, accompanied by a decrease of the L_3/L_2 intensity ratio and changes in the lineshape [38–41]. The Mn spectrum taken inside the electrolyte is very similar to the one for MnO [40], coherently with the 2 + valence of the salt dissolved in the solvent. The lineshapes and peak positions of the Mn spectra, measured within the cathode and anode areas, evidence the presence of different Mn oxidation states on the two electrodes. Compared to the spectrum recorded inside the electrolyte, the Mn spectrum from the cathode exhibits a shift to lower energy, accompanied by a decrease of the L_3/L_2 ratio, which indicates a partial reduction of Mn^{2+} to a lower valence state. On the contrary, the Mn spectrum measured at the anode clearly evidences that Mn^{2+} undergoes further oxidation at the anode with dominance of the Mn^{3+} state.

3.2. Electrochemical oxidation of electrodeposited Mn films

As mentioned in the Introduction, in this research we follow the literature approach of forming Mn oxide films by electrochemical oxidation of electrodeposited Mn layers [18–20]. In this Section we shall describe the electrochemical oxidation procedure as well as the electrical and optical characterisation of the materials we obtained. It is worth recalling that, from the thermodynamic point

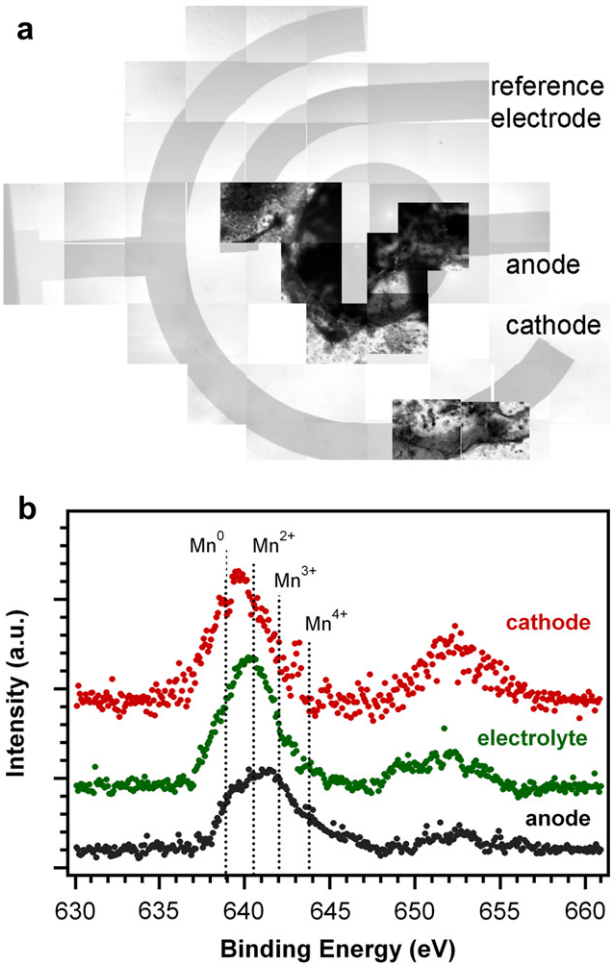

Fig. 3. (a) STXM images of the cell with Au anode and cathode after the application of a cathodic polarisation of −1.7 V for 2 min. (b) Mn $L_{3,2}$ absorption spectra taken in the positions of the anode (A), cathode (C) and electrolyte (E), as indicated in Fig. 3a.

of view [42], Mn can be oxidised to Mn^{2+}, Mn_3O_4, Mn_2O_3, and MnO_2 as a function of potential in a neutral aqueous solution.

3.2.1. Electrochemical measurements

Literature reports indicate that the best results in terms of capacitive behaviour of the Mn oxide grown by oxidation of Mn electrodeposits, are obtained using the CV method rather than potentiostatic and galvanostatic ones [19,43]. Fig. 4 describes the oxidation of a Mn film electrodeposited at −1.7 V, obtained with 40 voltammetric cycles at a scan rate of 25 mV s^{-1} in a 0.1 M Na_2SO_4 aqueous solution, with the initial and final potentials chosen according to [19]. An irreversible anodic c.d. branch is observed, that evidently decreases after the first CV cycles, indicating that Mn is gradually oxidised, until a steady cycle is obtained, highlighted in red. Fig. 4, also reveals that the anodic and cathodic charges involved in the anodic- and cathodic-going scans tend to become equal with increasing cycle number, denoting that a stable Mn oxide is formed. The nearly rectangular shape and the symmetry with respect to the potential axis of the CV curves observed after 40 scan cycles witness the notable reversibility and sound capacitive performance of the Mn oxide obtained with the adopted procedure.

3.2.2. In situ visible electroreflectance measurements

In situ reflectivity experiments have been carried out in order to monitor the oxide growth, by following the optical properties of the

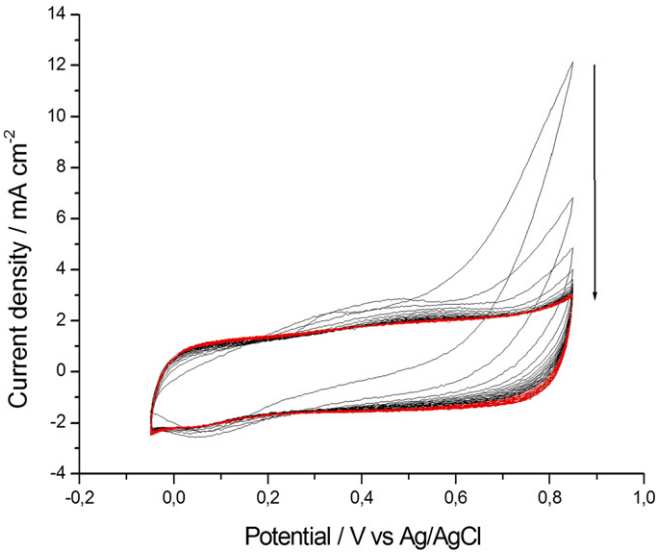

Fig. 4. Cyclic voltammograms (40 cycles, 25 mV s^{-1}) measured during the controlled oxidation in 0.1 M Na_2SO_4 aqueous solution of electrodeposited Mn film. The arrow indicates the evolution of the voltammetric curves as the number of cycles increases.

electrodeposited Mn film during electrochemical oxidation. The wavelength of 500 nm was chosen, were the difference among the reflectivity of different Mn oxides is maximal [44]. Fig. 5a shows the potential-dependent reflectivity (R) of the sample recorded during 40 cycles of voltammetry scans at 25 mV s^{-1}, (see Section 3.2.1) in the Na_2SO_4 solution. Each cycle varies between two levels of reflectivity R: a higher one close to the cathodic terminal potential and a lower one in the neighbourhood of the anodic terminal potential. Furthermore, R exhibits a systematic increase during the oxidation cycles until an asymptotic response is attained. According to literature data [20,44,45] and coherently with the applied polarisations, these levels correspond to trivalent and tetravalent states of manganese (i.e. to Mn_2O_3 and MnO_2 stoichiometries), at the lowest and highest potentials, respectively.

In order to more fully characterise the potential dependence of the oxide film reflectivity, after completion of the voltammetric oxidation, we applied a square wave polarisation of the potential, switching between the two values corresponding to the terminal voltages of the cycle (−50 and +850 mV): after an exponential transient, an asymptotic value of reflectivity is reached cyclically (Fig. 5b). This experiment shows that the potential-dependent conversion between the two types of oxide is reversible, though with individual relaxation times (estimated by fitting the experimental data with first order exponential growth and decay) of 205 ± 50 and 440 ± 50 s for the Mn(III) and Mn(IV) forms, respectively.

3.3. Characterization of electrochemically grown Mn oxide films

This Section described the characterisation of the oxide films in terms of their morphology and capacitance.

3.3.1. SEM morphology

The morphology of the Mn deposit obtained potentiostatically at −1.7 V for 1 h and anodized as described above was examined by SEM (Fig. 6). The formation of nanowires can be observed: this type of structure has been correlated with the excellent capacitive performance of the Mn oxide [18,46]. It is worth noting that manganese oxide nanowires [46] and nanotubes [47] – synthesized by electrodeposition followed by voltammetric oxidation

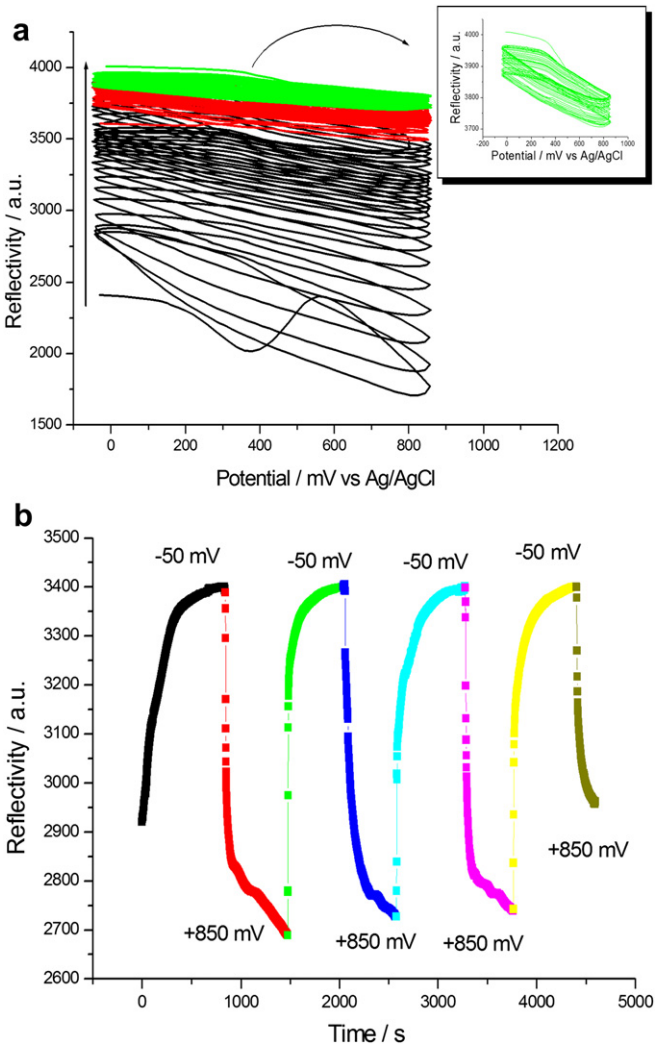

Fig. 5. (a) Potential-dependent p-polarised reflectivity at 500 nm recorded in situ during voltammetric oxidation of a Mn film electrodeposited at −1.7 V for 1 h 40 voltammetric cycles at 25 mV s^{-1}, in a 0.1 M Na_2SO_4 aqueous solution. (b) Reflectivity transients at 500 nm obtained by switching the potential between −50 and +850 mV after the oxidation process described in panel (a).

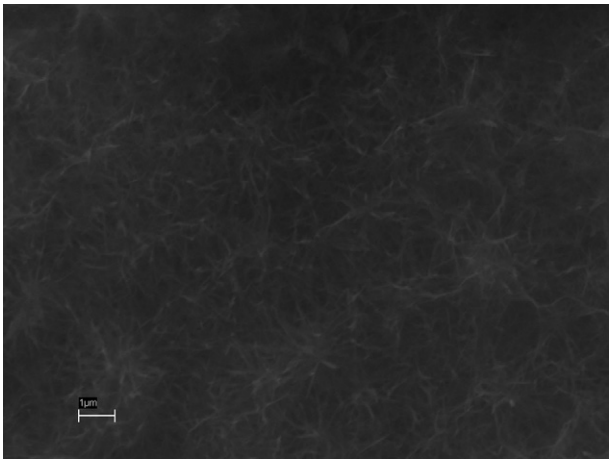

Fig. 6. SEM micrograph of the Mn film electrodeposited from the urea/ChCl bath at −1.7 V for 1 h and oxidised in 0.1 M Na_2SO_4 aqueous solution.

without surfactant, catalyst or template – have been reported in the literature.

3.3.2. Capacitance measurements

The capacitance of the electrochemically grown and oxidised films has been measured by electrochemical methods: CV and EIS. These methods are customarily used in the literature to examine the electrochemical properties of MnO_2 for supercapacitor [18–20,48]. Fig. 7a shows the CVs of anodised Mn electrodes at different scan rates from 5 to 100 mV s^{-1}. The approximately rectangular shape of the CV curves reveals the good capacitive characteristics of the Mn oxides prepared in this study. As described in the literature [18], the enclosed area of the CV curves, which corresponds to the charge storage capacity of the oxide electrodes, depends strongly on the material properties and thus on the Mn deposition conditions. To quantitatively evaluate the functional performance of the Mn oxides for perspective supercapacitor applications, the specific (i.e. referred to 1 g of oxide) capacitance C of the oxide electrode was estimated using the following equation [18,20]:

$$C = \frac{\text{specific voltammetric charge}}{\text{potential range}}$$

where the specific (i.e. referred to 1 g of oxide [18,20]) voltammetric charge was integrated from the positive and negative sweeps of the CV curves. Fig. 7b summarizes the specific capacitance of the various Mn oxides measured at the different investigated scan rates. The error bars were computed from triplicated experiments carried out with independently grown films; results for Mn electrodeposition in n-butylmethylpyrrolidinium bis(trifluoromethylsulfony)imide (BMP–NTf2) [18–20] are also shown. For consistency with the literature, we used the customary data presentation format. Moreover, the comparison between our results and literature data [18–20] has been shown also in terms of capacitance per unit geometric area (C_a) of the oxide electrode, estimated using the following equation [19]:

$$C_a = \frac{\text{voltammetric charge per unit electrode area}}{\text{potential range}}$$

where the voltammetric charge was integrated from the positive and negative sweeps of the CV curves. Our results compare favourably with literature figures and suggest that the material prepared by the approach proposed in the present work may be suitable for supercapacitor applications. It is worth noting that the capacitance can be extracted straightforwardly and perhaps in a physically more transparent way, from the same data by linear fitting of the CV area per unit electrode area vs. the scan rate v_s [49,50]. The capacitance values estimated by this approach are 632 ± 18 F g^{-1} (69.6 ± 2.0 mF cm^{-2}) for the Mn oxides obtained in this work and from 210 to 250 F g^{-1} (21–25 mF cm^{-2}) for literature data [18–20].

The capacitance of Mn oxide films was evaluated also by means of EIS. Impedance experiments were performed in the frequency range from 65 kHz to 1 MHz, with a sinusoidal potential modulation of 10 mV peak-to-peak and a bias of 400 mV, corresponding to the centre of the flat region of CVs. EIS results were interpreted in terms of the equivalent circuit model shown in Fig. 8a [51]: C is the capacitance and R_1 and R_2 represent the uncompensated electrolyte resistance and the charge transfer resistance of Faradaic processes, respectively. Fig. 8b shows the data measured with the Mn oxide resulting from four independent deposits. The experimental values and the fitting curve for the real and imaginary parts of the impedance as a function of frequency are reported. The NLLS estimate of the capacitance was 575 ± 101 F g^{-1} (63.3 ± 11.2 mF cm^{-2}), accurately matching the estimate obtained by the CV method.

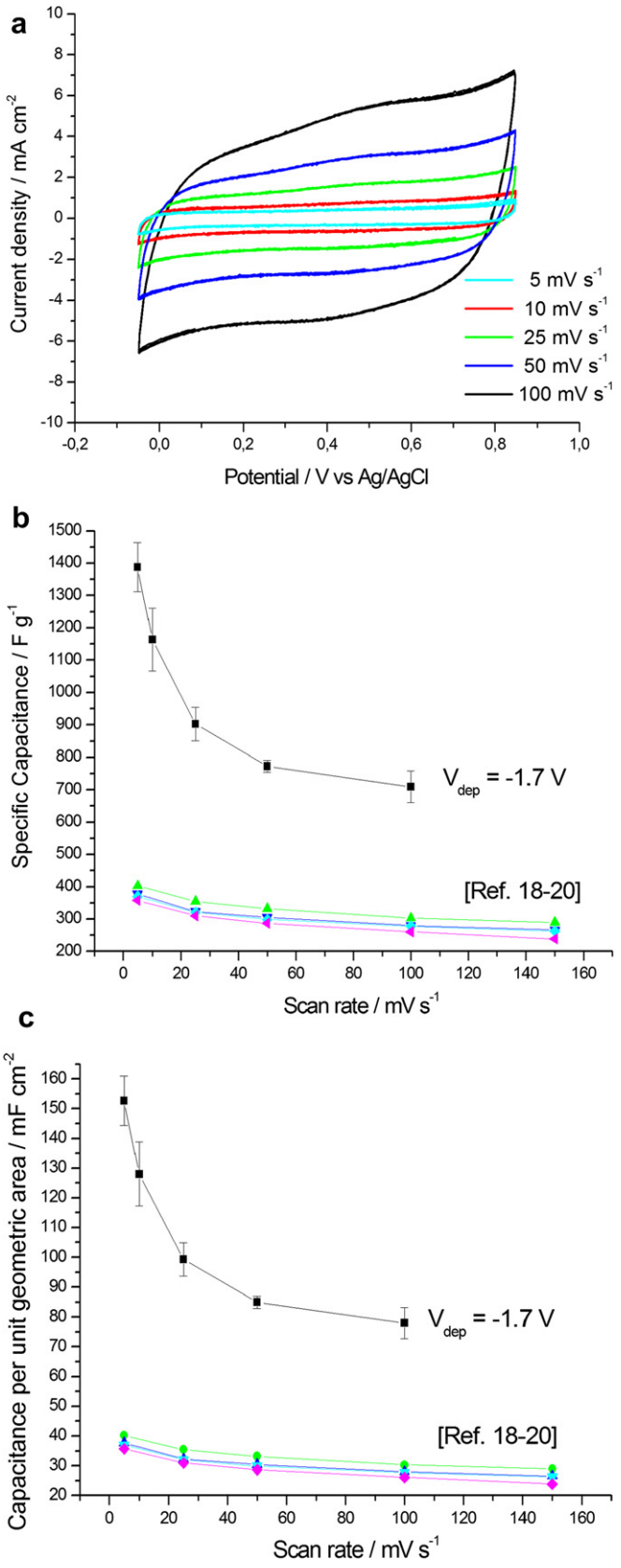

Fig. 7. (a) Cyclic voltammograms of oxidised Mn electrodes, measured in 0.1 M Na_2SO_4 aqueous solution, at the indicated scan rates. (b) Specific Capacitance as a function of the scan rate vs and comparison with literature data.

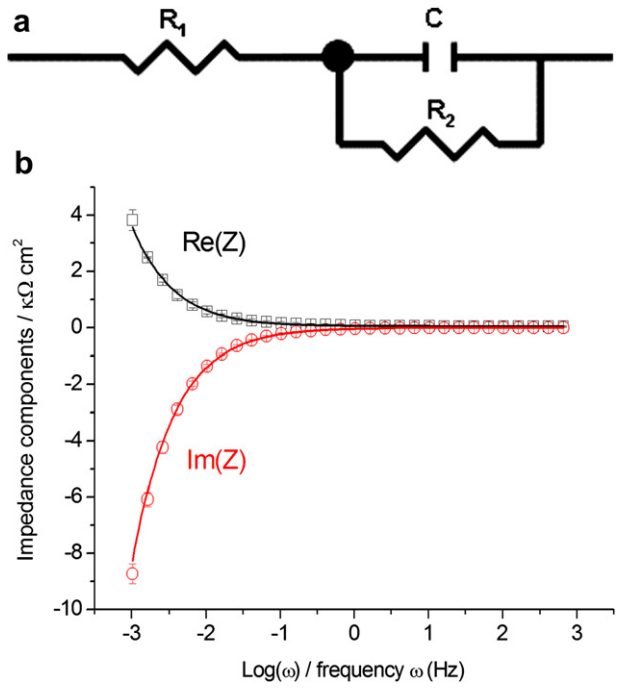

Fig. 8. (a) The equivalent circuit model used for the interpretation of electrochemical impedance spectra measured with Mn oxide films in contact with a 0.1 M Na_2SO_4 aqueous solution. (b) Real and imaginary parts of the measured impedance as a function of frequency: the symbols represent experimental data averaged over four replicated measurements with three independent material samples (error bars corresponding to one standard deviation), the continuous lines are the fits with the model corresponding to the equivalent circuit of Panel (a).

4. Conclusions

In this paper, we report a multi-method investigation of the electrodeposition of manganese from an eutectic choline chloride/urea ionic liquid, followed by electrochemically controlled oxidation in aqueous environment. The electrodeposition process was followed by synchrotron-based STXM and XAS spectromicroscopy experiments, that have yielded combined morphochemical information highlighting the space distribution of electrodeposited material and the corresponding chemical state of Mn. The electrochemical oxidation of the Mn deposits has been carried out by cyclic voltammetry and monitored in situ by visible electroreflectance measurements: good correlations were obtained between the applied potentials and the optical properties corresponding to different Mn oxidation states. The morphology of the oxide films was found to be of the nanowire type. The capacitance of the obtained films was been measured by CV and EIS, and yielded a value of 632 F g^{-1}, comparing extremely favourably with MnO_2 films grown by cognate methods.

Acknowledgments

Expert assistance with electrochemical experiments of Mr. Biagio Gennaro is gratefully acknowledged.

References

[1] B.E. Conway, Electrochemical Supercapacitors, Kluwer-Plenum, New York, 1999.
[2] E. Frackoviak, F. Béguin, Carbon 39 (2001) 937–950.
[3] C. Lin, B.N. Popov, H.J. Ploehn, J. Electrochem. Soc. 149(82002) A167–A175.
[4] D. Villers, D. Jobin, C. Soucy, D. Cossement, R. Chahine, L. Breau, D. Bélanger, J. Electrochem. Soc. 150 (2003) A747–A752.
[5] F. Fusalba, N. El Mehdi, L. Breau, D. Bélanger, Chem. Mater. 12 (2000) 2581–2589.
[6] J.P. Zheng, T.R. Jow, J. Electrochem. Soc. 142 (1995) L6–L8.
[7] P. Soudan, J. Gaudet, D. Guay, D. Bélanger, R. Schulz, Chem. Mater. 14 (2002) 1210–1215.
[8] B.E. Conway, V. Birss, J. Wojtowicz, J. Power Sources 66 (1997) 1–14.
[9] N.-L. Wu, S.-Y. Wang, C.-Y. Han, D.-S. Wu, L.-R. Schiue, J. Power Sources 113 (2003) 173–178.
[10] N.-L. Wu, Mater. Chem. Phys. 75 (2002) 6–11.
[11] T. Brousse, D. Bélanger, Electrochem. Solid-State Lett. 6 (2003) A244–A248.
[12] M. Toupin, T. Brousse, D. Bélanger, Chem. Mater. 14 (2002) 3946–3952.
[13] M.-J. Deng, P.-Y. Chen, I.-W. Sun, Electrochim. Acta 53 (2007) 1931–1938.
[14] J.-K. Chang, M.-T. Lee, C.-W. Cheng, W.-T. Tsai, M.-J. Deng, Y.-C. Hsieh, I.-W. Sun, J. Mater. Chem. 19 (2009) 3732–3738.
[15] C.M. Krowne, Phys. Lett. A 374 (2010) 614–619.
[16] H. Zhang, G. Cao, Z. Wang, Y. Yang, Z. Shi, Z. Gu, Nanoletters 8 (2008) 2664–2668.
[17] F. Endres, D. MacFarlane, A. Abbott (Eds.), Electrodeposition from Ionic Liquids, Wiley-VCH, Weinheim (D), 2008, p. 143 299–304.
[18] J.-K. Chang, C.-H. Huang, W.-T. Tsai, M.-J. Deng, I.-W. Sun, P.-Y. Chen, Electrochim. Acta 53 (2008) 4447–4453.
[19] J.-K. Chang, C.-H. Huang, M.-T. Lee, W.-T. Tsai, M.-J. Deng, I.-W. Sun, Electrochim. Acta 54 (2009) 3278–3284.
[20] J.-K. Chang, C.-H. Huang, W.-T. Tsai, M.-J. Deng, I.-W. Sun, J. Power Sources 179 (2008) 435–440.
[21] A.P. Abbott, G. Capper, D. Davies, R.K. Rasheed, Chem. Eur. J. 10 (2004) 3769–3774.
[22] A.P. Abbott, K. El Ttaib, G. Grish, K.J. McKenzie, K.S. Ryder, Phys. Chem. Chem. Phys. 11 (2009) 4269–4277.
[23] R. Böck, S.-E. Wulf, Trans. Inst. Met. Finish. 87 (2009) 28–32.
[24] A. Bakkar, V. Neubert, Electrochem. Commun. 9 (2007) 2428–2435.
[25] A.P. Abbott, G. Capper, K. Mckenzie, K. Ryder, J. Electroanal. Chem. 599 (2007) 288–294.
[26] P. Dale, A. Samantilleke, D. Shivagan, L. Peter, Thin Solids Films 515 (2007) 5751–5754.
[27] B. Bozzini, A. Bund, B. Busson, C. Humbert, A. Ispas, C. Mele, A. Tadjeddine, Electrochem. Commun. 12 (2010) 56–60.
[28] S. Zein El Abedin, Electrochim. Acta 54 (2009) 5673–5677.
[29] B. Kaulich, J. Susini, C. David, E.Di Fabrizio, G. Morrison, P. Charalambous, J. Thieme, T. Wilhein, J. Kovac, D. Bacescu, M. Salome, O. Dhez, T. Weitkamp, S. Cabrini, D. Cojoc, A. Gianoncelli, U. Vogt, M. Podnar, M. Zangrando, M. Zacchigna, and M.Kiskinova, , in Proc. 8th Int. Conf. X-ray Microscopy (eds. S.Aoki, Y.Kagoshima, Y.Suzuki), Conf. Proc. Series IPAP vol. 7, pp. 22–25.
[30] B. Kaulich, P. Thibault, A. Gianoncelli, M. Kiskinova, J. Phys. Condensed Matter 23 (2011) 083002.
[31] B. Bozzini, L. D'Urzo, A. Gianoncelli, B. Kaulich, M. Prasciolu, I. Sgura, E. Tondo, M. Kiskinova, J. Phys. Chem. C 113 (2009) 9783–9787.
[32] B. Bozzini, A. Gianoncelli, B. Kaulich, M. Kiskinova, C. Mele, M. Prasciolu, Phys. Chem. Chem. Phys. 13 (2011) 7968–7974.
[33] A. Gianoncelli, G.R. Morrison, B. Kaulich, D. Bacescu, J. Kovac, Appl. Phys. Lett. 89 (2006) 251117–251119.
[34] G.R. Morrison, A. Gianoncelli, B. Kaulich, D.Bacescu, J.Kovac: , in Proc. 8th Int. Conf. X-ray Microscopy (eds. S.Aoki, Y.Kagoshima, Y.Suzuki), Conf. Proc. Series IPAP vol. 7, 377–379.
[35] B. Bozzini, C. Mele, A. Gianoncelli, B. Kaulich, M. Kiskinova, M. Prasciolu, Microelectron. Eng. 88 (2011) 2456–2458.
[36] B. Bozzini, A. Gianoncelli, B. Kaulich, M. Kiskinova, M. Prasciolu, I. Sgura, Chem. Sus. Chem. 7 (2010) 846–850.
[37] A. Gianoncelli, B. Kaulich, M. Kiskinova, M. Prasciolu, L.D. Urzo, B. Bozzini, Micron 42 (4) (2011) 342–347.
[38] M.M. Grush, J. Chen, T.L. Stemmler, S.J. George, C.Y. Ralston, R.T. Stibrany, A. Gelasco, G. Christou, S.M. Gorun, J.E. Penner-Hahn, S.P. Cramer, J. Am. Chem. Soc. 118 (1996) 65–69.
[39] S. Kobayashi, I.R.M. Kottegoda, Y. Uchimoto, M. Wakihara, J. Mater. Chem. 14 (2004) 1843–1848.
[40] L. Chow, A. Misiuk, C.W. Pao, D.C. Ling, W.F. Pong, J. Bak-Misiuk, VIII KSUPS 2009: Abstr./Synchrotron Radiat. Nat. Sci. 8 (1–2) (2009).
[41] B. Gilbert, B.H. Frazer, A. Belz, P.G. Conrad, K.H. Nealson, D. Haskel, J.C. Lang, G. Srajer, G. De Stasio, J. Phys. Chem. A 107 (2003) 2839–2847.
[42] M. Pourbaix, Atlas of Electrochemical Equilibria in Aqueous Solutions, National Association of Corrosion Engineers, TX, USA, 1966.
[43] M.-S. Wu, P.-C.J. Chiang, Electrochem. Solid-State Lett. 7 (2004) A123–A126.
[44] S. Eckhoff, I. Alxneit, M. Musella, H.-R. Tschudi, Development of a Reflectometer for the Determination of the Spectral Emittance in the Visible at High Temperatures, in PSI Scientific Report – Annex V, Paul Scherrer Institut, Villigen, Switzerland, 2000, 26–28.
[45] J.-K. Chang, M.-T. Lee, W.-T. Tsai, H.-F. Cheng, I.-W. Sun, Langmuir 25 (2009) 11955–11960.
[46] M. Wu, Appl. Phys. Lett. 87 (2005) 153102.
[47] M. Wu, J.-T. Lee, Y.-Y. Wang, C.-C. Wan, J. Phys. Chem. B 108 16331–16333.
[48] C. Ye, Z.M. Lin, S.Z. Hui, J. Electrochem. Soc. 152 (2005) A1272–A1278.
[49] J.P. Zheng, C.M. Pettit, P.C. Goonetilleke, G.M. Zenger, D. Roy, Talanta 78 (2009) 1056–1062.
[50] C.E. Banks, A. Crossley, C. Salter, S.J. Wilkins, R.G. Compton, Angew. Chem. 118 (2006) 2533–2537.
[51] M. Ghaemi, F. Ataherian, A. Zolfaghari, S.M. Jafari, Electrochim. Acta 53 (2008) 4607–4614.